



# CHORUS

This is the accepted manuscript made available via CHORUS. The article has been published as:

## Spectroscopic observation of bound ungerade ion-pair states in molecular hydrogen

R. C. Ekey, Jr. and E. F. McCormack

Phys. Rev. A **84**, 020501 — Published 22 August 2011

DOI: [10.1103/PhysRevA.84.020501](https://doi.org/10.1103/PhysRevA.84.020501)

# Spectroscopic observation of bound *ungerade* ion-pair states in molecular hydrogen

R. C. Ekey, Jr.

University of Mount Union, Alliance, OH 44601

E. F. McCormack\*

Bryn Mawr College, Bryn Mawr, PA 19010

Frequency-resolved observations of heavy Rydberg states in molecular hydrogen are reported for the first time in the *ungerade* manifold of states. Double resonance spectroscopy via the E,F  $1\Sigma_g^+$ ,  $v'=6$  state has been used to probe the energy region above the  $H(1s) + H(3l)$  dissociation threshold. Resonances are observed by ionizing  $H(3l)$  to produce  $H^+$ , which is then detected by using a time-of-flight mass spectrometer. The kinetic energy of the  $H^+$  ion confirms that the observed signal is due to the photo-ionization of neutral  $H(3l)$  atoms, indicating that dissociation is a significant decay channel for the ion-pair states. The pattern of energies of the resonances agree well with the predictions of a mass-scaled Rydberg formula for bound quantum states of the  $H^+ H^-$  ion-pair. Energies and quantum defects have been determined for principal quantum numbers in the range of  $n=130$  to 207.

PACS numbers: 32.80.Ee, 03.65.Ge, 33.80.Eh

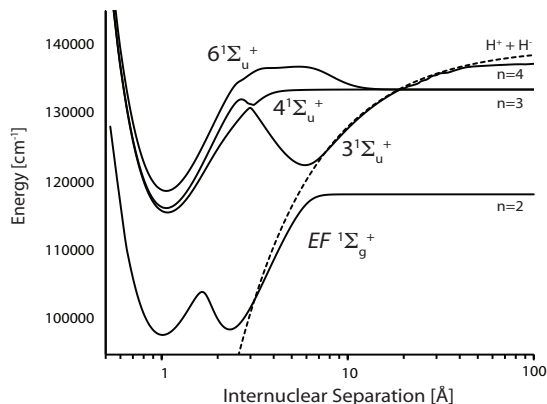


FIG. 1. Potential energy curves of select *ungerade* double-well states in  $H_2$ . [5, 6] The  $H^+H^-$  ion-pair Coulombic potential curve is shown as a dotted line. The *gerade* E,F  $1\Sigma_g^+$  state is shown for comparison.

The hydrogen molecule, being the simplest stable neutral molecule, is an important system for investigating our understanding of photodynamical processes such as photoionization, photodissociation, ion-pair formation and photo-association in molecules. The structure and dynamics of its energy levels continues to be a significant test of *ab initio* and semi-empirical methods used to describe super-excited molecular configurations where internal energies exceed ionization and dissociation thresholds and large ranges of internuclear separation must be taken into account. [1, 2] The dynamics of highly excited states of  $H_2$  are of interest to many areas of research. For example, since most of the interstellar medium is in the form of  $H_2$ , the mechanisms and rates of its transformation mediated through excited-state configurations are

key to understanding many astrophysical environments including cold molecular clouds and star forming regions in space. [3, 4]

*Ab initio* calculations of the 3-6  $1\Sigma_u^+$  *ungerade* potential energy curves which correlate to the third and fourth dissociation limits predict double-well configurations that support bound states of exceptionally large size. [5, 6] Double-well long-range state configurations are produced by avoided crossings between multiple electronic potential energy curves. At relatively small internuclear separation, the inner well is formed by an avoided crossing between a bound molecular state and a doubly-excited dissociative state, and at large internuclear separation, the outer well is formed by a crossing with the ion-pair configuration. As shown in Fig. 1, members of the series of  $1\Sigma_u^+$  electronic states closely follow the ion-pair potential in large sections of their outer wells. [7]

The unusual structure and dynamics of these molecular configurations have long been of interest, however these same attributes have also made them difficult to study. [8–11] In particular, the ion-pair configuration has yet to be fully explored in molecular hydrogen. In a typical interaction between two neutral hydrogen atoms with internuclear separation  $r$ , the lowest-order power-law interaction that can exist between the atoms is  $1/r^3$ , which leads to a finite number of vibrational motions between the two atoms. For the case of the ionic interaction however between an ion pair such as  $H^+$  and  $H^-$  the binding is Coulombic and leads to an infinite series of vibrational modes that behave like the electronic Rydberg states of the Bohr atom, although characterized by a much heavier reduced mass,  $\mu = (1/2)M_H$ , where  $M_H$  is the mass of the hydrogen atom. [12] Ion-pair state energies,  $E_n$ , can be calculated by using a heavy Bohr atom model of the  $H^+H^-$  system.

\* emccorma@brynmawr.edu

$$E_n = E_{IP} - \frac{R_{IP}}{(n - \delta)^2} \quad (1)$$

Here  $n$  is the principal quantum number and  $\delta$  is the quantum defect for the heavy Rydberg series. The ion-pair dissociation limit for molecular hydrogen,  $E_{IP}$ , is  $139713.83 \text{ cm}^{-1}$ . The ion-pair Rydberg constant,  $R_{IP}$ , is obtained by scaling the infinite mass Rydberg constant,  $R_\infty$  by the reduced mass of the ion pair,  $\mu = 918.5761$ . [12]

The energy region of the ion-pair limit has been investigated previously producing a variety of results including the development of threshold ion-pair production spectroscopy (TIPPS) [13] and a time-domain method of studying the threshold region using coherent ion-pair wavepacket excitation in electric fields. [14] Direct observation of bound ion-pair states in the frequency domain however has been challenging because the  $\text{H}^-$  ion is very diffuse and stable ion-pair states only exist at very large internuclear separations greater than  $7 \text{ \AA}$ . [15] Early attempts to directly observe bound ion-pair states in  $\text{H}_2$  were made through excitation of intermediate states with average internuclear separations less than  $5 \text{ \AA}$ . [16–18] These studies found the spectra dominated by relatively short-range electronic molecular states. It was only recently that Vieitez *et al.* observed for the first time spectral features corresponding to bound ion-pair states by using a laser-based XUV light source in a two-photon excitation scheme. [19, 20] Consistent with the earlier investigations, the ion-pair resonances were observed in the photo-excitation yield of  $\text{H}_2^+$  ions due to the strong coupling with short-range electronic molecular states. These results prompted new theoretical work by Kirrander on  $\text{H}_2$  to predict more accurately ion-pair resonance energies and widths and their perturbations by near-by molecular states with *gerade* symmetry. [21]

Here we report the first observation of the ion-pair series subject to interactions with *ungerade* states and detected through the interaction of these states with a neutral dissociative channel. We have determined the energies and quantum defects for bound states of the ion-pair series with principal quantum numbers in the range of  $n=130$  to 207. In agreement with the new theoretical results of Kirrander for the *gerade* symmetry, we observe a strongly varying quantum defect for the series and evidence of perturbations due to interloping states.

Double resonance spectroscopy via the  $\text{E,F } ^1\Sigma_g^+, v'=6$  state is used to probe the energy region above the  $\text{H}(1s) + \text{H}(3l)$  dissociation threshold. Resonances are observed by ionizing neutral  $\text{H}(3l)$  to produce  $\text{H}^+$ , which is then detected by using a time-of-flight mass spectrometer. Fig. 2 illustrates the apparatus used to acquire ionization spectra. [10] Narrow bandwidth radiation at 193 nm is generated by frequency mixing the output of a 704-nm pulsed dye laser with the output of the fourth harmonic of a Nd:YAG laser at 266 nm and used to populate the  $v'=6$  level of the  $\text{E,F } ^1\Sigma_g^+$  state by two-photon absorption from the ground state. From the  $\text{E,F } ^1\Sigma_g^+$  state molecular valence, Rydberg and ion-pair states between the  $n=3$  and  $n=4$  dissociation limits can be reached with an additional single photon produced by a second Nd:YAG pumped tunable dye laser system.

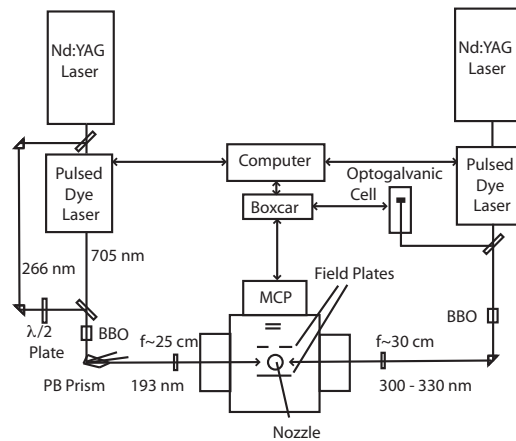


FIG. 2. Schematic of the experimental arrangement. The laser set-up depicted on the left is used to generate pump light pulses at 193 nm. The laser set-up shown on the right is used to generate probe light pulses in the wavelength range of 300-330 nm.

A collision-free beam of molecular hydrogen is produced by using a supersonic expansion of pure  $\text{H}_2$  from a solenoid-driven pulsed valve. Counter-propagating pump and probe light pulses cross the molecular beam in the interaction region located between two electric field plates, across which a voltage can be applied to accelerate ions towards a multi-channel plate detector. A time delay of 40 ns is introduced between the pump and probe pulses to distinguish ions produced by the pump beam alone and those produced by two-color resonant excitation. Ions generated by the two-color process are accelerated into the time-of-flight mass spectrometer by a pulsed electric field of 125 V/cm. Probe spectra are acquired by fixing the frequency of the pump light and scanning the frequency of the probe light. Spectra are produced by scanning the frequency of the probe light while monitoring the production of  $\text{H}^+$  ions by using a boxcar integrator with a timed gate set to collect the ions of interest. The optogalvanic effect in several elements and a wavemeter are used to calibrate the probe laser wavelength. Total energies are referenced to the  $\text{X } ^1\Sigma_g^+, v''=0$  state ground state by using the known  $\text{E,F } ^1\Sigma_g^+, v'=6$  transition energies [22] and ground state and  $\text{E,F } ^1\Sigma_g^+, v'=6$  state rotational intervals. [23]

Fig. 3 displays the spectrum of the  $\text{H}^+$  ion yield as a function of total energy. Note the regular pattern of the resonance positions with energy. These are compared in the upper portion of the figure with the expected energies of accessible electronic Rydberg states in this energy region. These are denoted as  $npN^+, v^+$ , indicating the excitation of a  $p$  electron with electronic principle quantum number,  $n$ , bound to an  $\text{H}_2^+$  core with angular momentum  $N^+$  and  $v^+$  quanta of vibration. [24] The predicted energies of the ion-pair series,  $n_{IP}$ , based on Eq. (1) with the quantum defect  $\delta$  set to zero are shown in the lower portion of Fig. 3. Note that the predicted

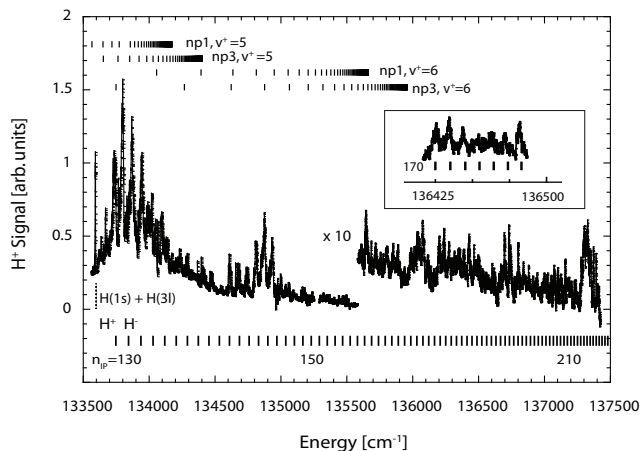


FIG. 3.  $H^+$  yield as a function of energy, above the  $H(1s) + H(3l)$  dissociation limit, obtained by excitation from the  $E,F \ ^1\Sigma_g^+$ ,  $v'=6$ ,  $J'=1$  state. The signal is magnified at high energy to show more detail. The insert provides an expanded view showing an example of the regular pattern of resonances observed at high energy.

convergence with energy of the possible electronic Rydberg states cannot account for the dominant pattern of resonances observed in the spectrum. The relative spacing of the calculated ion-pair levels and their convergence with energy however, are a good match to the observed resonances.

An assignment of the observed features to the ion-pair series is further supported by a consideration of the origin of the  $H^+$  signal in the experiment illustrated in Fig. 4. Once excited to the  $E,F \ ^1\Sigma_g^+$ ,  $v'=6$  state, the molecule can absorb a probe photon and produce  $H^+$  via two distinct pathways. First, shown as a), the molecular ion can be created in a dissociative state which then decays into  $H$  and  $H^+$  with each fragment possessing an equal amount of kinetic energy. Alternatively, shown as b), the molecule can absorb a single photon and dissociate into two neutral atoms,  $H(1s) + H(3l)$ . The  $H(3l)$  atom can then absorb an additional probe photon to produce  $H^+$  ions with a relatively small amount of kinetic energy compared to the a) process. In the time-of-flight apparatus the relative difference in kinetic energy of the  $H^+$  ions is detected as a difference in the width of the  $H^+$  time-of-flight profile. A comparison of the  $H^+$  time-of-flight profile for bound electronic Rydberg states located in energy below the  $H(1s) + H(3l)$  threshold, where process b) cannot occur, with the  $H^+$  time-of-flight profile from excitation of the  $H(1s) + H(3l)$  continuum, allows us to distinguish electronic Rydberg excitation from neutral dissociation. From the time-of-flight profile of the  $H^+$  signal corresponding to the ion-pair features, it is clear the signal results from process b) and that the ion-pair series is significantly coupled to the neutral dissociation channel. This coupling mechanism explains the presence of ion-pair resonances in the spectrum of  $H^+$  yield.

A best fit of Eq. (1) to the observed peak energies

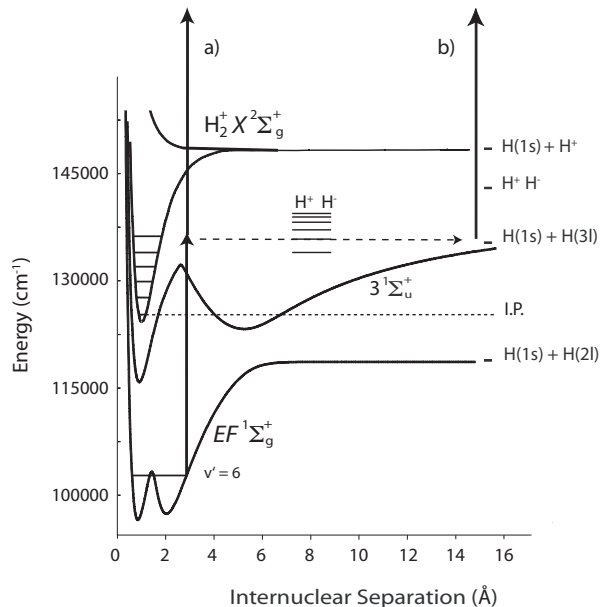


FIG. 4. Excitation and dynamics that lead to the production of  $H^+$  ions from the excitation of the  $E,F \ ^1\Sigma_g^+$ ,  $v'=6$ ,  $J'=1$  state. a) Dissociation of the molecular ion. b) Ionization of the  $H(3l)$  atomic fragment.

provides a quantum defect value of  $\delta = -0.08 \pm 0.04$ . This result can be compared with the value reported by Vieitez and coworkers,  $\delta = 0.05$  obtained from a fit of the *gerade* members of the series in the range of  $n=161$  and  $230$ . [19] While the results appear to be in disagreement, the new theoretical results from Kirrander explain the apparent discrepancy. Upon close examination of the fit, a systematic variation with  $n$  suggests the series is not described well by a constant quantum defect, but rather by one that is increasing with principal quantum number. Kirrander's calculations confirm that this behavior is indeed expected because the ion-pair states in this energy region have not yet reached large enough internuclear separations that would result in a constant value of  $\delta$ . [21]

Guided by the new theoretical results, the observed resonances can be assigned a principal quantum number and individual quantum defects calculated. These are shown in Fig. 5. The wide variation and nearly linear trend with energy of the quantum defects is similar to the results for the *gerade* series. Excitation from the  $E,F \ ^1\Sigma_g^+$ ,  $v'=6$ ,  $J'=1$  state to the  $J=0$  and  $J=2$  levels of the ion-pair series are expected to be populated, however the width of the observed resonances, which range from  $5 - 35 \text{ cm}^{-1}$ , limits our ability to resolve levels more closely spaced than the observed widths. The results of Kirrander for the *gerade* series suggest the energy spacing between different  $J$  levels is too small to be observed here.

In the excitation scheme used here, levels of *ungerade*

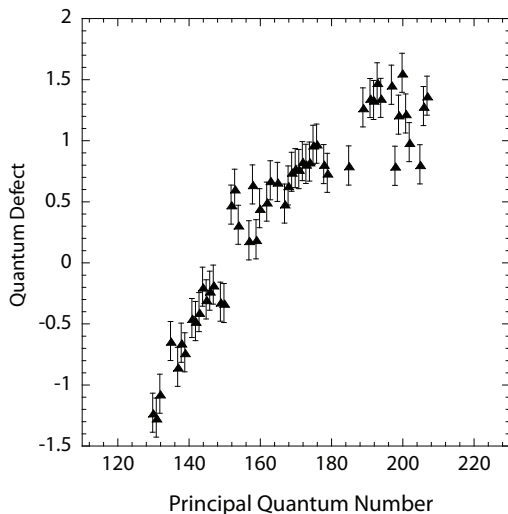


FIG. 5. Observed quantum defects as a function of assigned ion pair principal quantum number. The error bars are the standard deviation of a fit of the variation of the quantum defect to a linear dependence on energy.

symmetry are accessed and a different set of interlopers from those predicted for the *gerade* series are expected. As can be seen in both Fig. 3 and Fig. 5, at  $n=150$  and again at  $n=180$  the series is visibly disrupted and may indicate the presence of interloping states. Candidates for such interlopers include the high vibrational levels of the sigma series of states shown in Fig. 1 and the

electronic molecular Rydberg states shown in Fig. 3.

Spectra have also been acquired through excitation of the  $J'=0$  and 2 levels of the E,F  $1^1\Sigma_g^+$ ,  $v'=6$  state. These spectra also exhibit resonances attributable to members of the ion-pair series. A comparison of the observed ion-pair series and their perturbation as a function of total angular momentum will help identify possible interloping states and such an analysis will be the subject of a longer publication.

Frequency-resolved observations of long-range ion-pair configurations in molecular hydrogen have been observed for the first time in the *ungerade* manifold of states. The results indicate a strong coupling of the series to the  $n=3$  dissociation continuum. A rapidly varying quantum defect has been observed for the series between  $n=130-207$  and evidence of perturbations to the series indicate the presence of interloping states. Further experimental and theoretical investigations of the series' interactions with other short and long-range states and the coupling mechanisms involved in the detection of ion-pair resonances will inform our understanding of this fundamental example of a heavy Bohr atom.

#### ACKNOWLEDGMENTS

This work was supported by a grant from the National Science Foundation (PHY-0140296). The authors would also like to thank Yingzi Wang, Emma Wisniewski-Barker and Clarah Lelei for their contributions to this project.

- 
- [1] N. Kouchi, M. Ukai, and Y. Hatano, *J. Phys. B: At. Mol. Opt. Phys.* **30**, 2319 (1997).
- [2] M. Glass-Maujean, C. Jungen, and H. Schmoranzer, *Phys. Rev. Lett.* **104**, 183002 (2010).
- [3] G. Shaw, G. J. Ferland, N. P. Abel, P. Stancel, and P. A. M. V. Hoof, *Astrophys. J.* **624**, 794 (2005).
- [4] K. Kreckel, H. Bruhns, M. Cizek, S. C. O. Glover, K. A. Miller, X. Urbain, and D. Savin, *Science* **329**, 69 (2010).
- [5] G. Staszewska and L. Wolniewicz, *J. of Mol. Spec.* **212**, 208 (2002).
- [6] T. Detmer, P. Schmelcher, and L. S. Cederbaum, *J. Chem. Phys.* **109**, 9694 (1998).
- [7] G. Corongiu and E. Clementi, *J. Phys. Chem. A* **113**, 14791 (2009).
- [8] A. de Lange, W. Hogervorst, W. Ubachs, and L. Wolniewicz, *Phys. Rev. Lett.* **86**, 2988 (2001).
- [9] J. C. J. Koelemeij, A. de Lange, and W. Ubachs, *Chem. Phys.* **287**, 349 (2003).
- [10] R. C. Ekey, J. A. Marks, and E. F. McCormack, *Phys. Rev. A* **73**, 023412 (2006).
- [11] M. Glass-Maujean, S. Klump, L. Werner, and a. H. S. A. Ehresmann, *J. Chem. Phys.* **126**, 144303 (2007).
- [12] E. Reinhold and W. Ubachs, *Mol. Phys.* **103**, 1329 (2005).
- [13] R. C. Shiell, X. Hu, Q. Hu, J., and J. Hepburn, *Faraday Discuss.* **115**, 331 (2000).
- [14] E. Reinhold and W. Ubachs, *Phys. Rev. Lett.* **88**, 013001 (2001).
- [15] M. L. Du, *Phys. Rev. A* **40**, 1330 (1989).
- [16] W. A. Chupka, P. M. Dehmer, and W. T. Jivery, *J. Chem. Phys.* **63**, 3929 (1975).
- [17] S. T. Pratt, E. F. McCormack, J. L. Dehmer, and P. M. Dehmer, *Phys. Rev. Lett.* **68**, 584 (1992).
- [18] A. H. Kung, R. H. Page, R. J. Larkin, Y. R. Shen, and Y. T. Lee, *Phys. Rev. Lett.* **56**, 328 (1986).
- [19] M. O. Vieitez, T. I. Ivanov, E. Reinhold, C. A. de Lange, and W. Ubachs, *Phys. Rev. Lett.* **101**, 163001 (2008).
- [20] M. O. Vieitez, T. I. Ivanov, E. Reinhold, C. A. de Lange, and W. Ubachs, *J. Phys. Chem. A* **113**, 13237 (2009).
- [21] A. Kirrander, *J. Chem. Phys.* **133**, 121103 (2010).
- [22] Y. P. Zhang, C. L. Gan, J. P. Song, X. J. Yu, H. Ge, R. Q. Ma, C. S. Li, K. Q. Lu, and E. E. Eyler, *Chinese Phys. Lett.* **22**, 1110 (2005).
- [23] G. H. Dieke, *J. of Mol. Spec.* **2**, 494 (1958).
- [24] S. T. Pratt, E. F. McCormack, J. L. Dehmer, and P. M. Dehmer, *The Journal of Chemical Physics* **92**, 1831 (1990).